International Journal of Mechanical, Industrial and Aerospace Sciences
ISSN: 2517-9950
Vol:7, No:4, 2013

Development of a Water-Jet Assisted Underwater Laser Cutting Process

Suvradip Mullick, Yuvraj K. Madhukar, Subhranshu Roy, and Ashish K. Nath

Abstract—We present the development of a new underwater laser cutting process in which a water-jet has been used along with the laser beam to remove the molten material through kerf. The conventional underwater laser cutting usually utilizes a high pressure gas jet along with laser beam to create a dry condition in the cutting zone and also to eject out the molten material. This causes a lot of gas bubbles and turbulence in water, and produces aerosols and waste gas. This may cause contamination in the surrounding atmosphere while cutting radioactive components like burnt nuclear fuel. The water-jet assisted underwater laser cutting process produces much less turbulence and aerosols in the atmosphere. Some amount of water vapor bubbles is formed at the laser-metal-water interface; however, they tend to condense as they rise up through the surrounding water. We present the design and development of a water-jet assisted underwater laser cutting head and the parametric study of the cutting of AISI 304 stainless steel sheets with a 2 kW CW fiber laser. The cutting performance is similar to that of the gas assist laser cutting; however, the process efficiency is reduced due to heat convection by water-jet and laser beam scattering by vapor. This process may be attractive for underwater cutting of nuclear reactor components.

Keywords—Laser, underwater cutting, water-jet.

I. Introduction

THE laser cutting in water environment has attracted much attention in recent years because of its several inherent advantages [1]-[9]. Lu et al. reported significant enhancements in the laser-drilling efficiency and quality in underwater drilling of different types of metal sheets by a Q-switched Nd: YAG laser [1]. Underwater laser processing provides a higher impact force and stronger shock wave because of the water confinement of laser produced plasma, intense liquid-jet-induced impulses due to bubbles collapse, and also better cooling. The phenomenon of strong shock wave generation in presence of a thin water layer has been exploited in laser shock peening process for introducing compressive stress into the workpiece surface to improve fatigue characteristics [10]. This can produce both higher depth and larger magnitude of residual stresses than the conventional shot peening process. Laser drilling, cutting and micromachining of brittle materials like glass, silicon wafer, silicon carbide and alumina, etc. carried out in water environment reportedly have a higher processing rate, efficient debris removal, better surface morphology and less thermal damages compared to that in air [2]-[9].

Water-assisted laser cutting of thin sheets with negligible thermal damages and dross deposition has been also developed for processing medical components [11], [12]. Synova S. A. Switzerland [13] has pioneered and patented a technology of water micro-jet guided laser cutting to process thin specimens in air. The laser beam is guided through a high pressure water micro-jet which facilitates a long working distance from the nozzle. This produces virtually no thermal and mechanical damages, negligible contamination and dross in cutting thin metal sheets, silicon wafer, and ceramic materials etc. [14], [15]. More recently, Tangwarodomnukun et al. [16] developed a hybrid laser water-jet ablation technology to minimize the thermal damages. In this process the target material, which is covered with a thin water layer, is heated and softened by a laser beam; and the softened material is expelled by a non-coaxial water-jet.

Underwater laser processing, viz. cutting, welding, cladding, and shock peening are often used in the maintenance, repairing and dismantling of nuclear reactor components [17]- [20]. Chida et al. developed a gas-assisted underwater laser cutting process to cut thick steel plates for applications in nuclear industry [17]. The high pressure gas jet used in the underwater cutting process produces a dry condition in the laser cutting zone and also removes the molten material from kerf. They reported cutting of 14 mm thick steel plate with minimal dross using an Nd: YAG laser at 4 kW power [17]. Based on this technique Jain et al. reported cutting 4.2 mm thick zircaloy pressure tubes and up to 6 mm thick steel using a fiber-coupled 250 W average power pulsed Nd:YAG laser [18]. Hino et al. reported the development of an underwater laser cladding and welding process for repairing stress corrosion cracks in nuclear reactor components [19]. In this technique also, a locally dried environment is created by a high pressure gas jet employed simultaneously with the laser beam. Kruusing et al. presented an exhaustive review of various schemes of gas-assisted and water-assisted underwater laser cutting processes; and described in detail the underwater cutting of nuclear fuel rods with high power CO_2 and Nd: YAG lasers [20].

In gas assisted underwater laser cutting, the high pressure gas produces high turbulence in water and aerosols as it bubbles out of water. In case of cutting radioactive materials the gas can carry some amount of radioactive particles along with it as aerosols and cause contamination in the surrounding

Suvradip Mullick, Yuvraj K. Madhukar, Subhranshu Roy, and Ashish K. Nath are with Department of Mechanical Engineering, Indian Institute of Technology, Kharagpur, West Bengal-721302, India, Corresponding Author: Ashish K. Nath (E-mail:suvradip.mullick@gmail.com(S.Mullick), uvraj.nit@gmail.com (Y.K Madhukar) suroy@iitkgp.ac.in (S. Roy), aknath@mech.iitkgp.ernet.in (A. K. Nath)).

atmosphere. In order to minimize the turbulence in water and the gas and aerosols emerging out of water, a water-jet assisted underwater laser cutting technique has been developed. In this technique a high speed water-jet has been used coaxially along with a high power fiber laser beam to remove molten material from the cutting front. AISI 304 steel sheets up to 1.5 mm thickness was cut at 1800 W CW laser power with the present experimental setup at a maximum cutting speed of 1.4 m/min with water-jet speed of 18 m/s. The water-jet reduced the turbulence in water considerably, but it increased the convective heat loss in the cutting process. Some amount of water vapor bubbles formed at the laser-metal-water interface and this caused scattering of the incoming laser beam. Since production of turbulence in water and aerosols in the surrounding environment are drastically reduced, this process may be attractive for cutting nuclear reactor components underwater. In this paper we present the designed and development of a water-jet assisted underwater laser cutting head and a parametric study of the underwater water-jet assisted laser cutting of AISI 304 stainless steel sheet carried out with a high power fiber laser.

II. Experimental Set-Up

The underwater laser cutting head which has been designed and developed is schematically shown in Fig. 1. This incorporates a plano-convex lens of 25 mm diameter and 25.4 mm effective focal length, an optical window and a nozzle of 1.5 mm orifice diameter. In underwater laser cutting of thick materials, high power CO_2 laser operating at 10.6 μm wavelength or Nd:YAG / fiber lasers operating at 1.06 μm / 1.07 μm wavelength are commonly used. The absorption coefficient of water at 10.6 μm and 1.06 μm /1.07 μm wavelengths is ~1000 cm^{-1} and ~0.135 cm^{-1}, respectively, therefore CO_2 laser beam gets readily absorbed within ~10 μm water column length, while Nd: YAG / fiber laser beam can travel up to ~75 mm before it gets attenuated by 67% [21], [22]. Because of the relatively low absorption of water at 1.07 μm wavelength, a 2 kW CW Yb-fiber laser has been used in the present experiments. The laser beam travels a distance of 13.7 mm through water inside the nozzle to reach the focal point. The laser focal point is nearly at 0.5 mm below the nozzle tip. The laser spot diameter, d_b at the focal plane was measured to be about 600 μm. The large focal spot diameter is mainly due to the spherical aberration of plano-convex lens (F no. 1) and the high divergence of laser beam which has a non-uniform intensity distribution [23]. The experimental setup consists of a centrifugal water pump of 3 bar maximum pressure head, a water tank and a processing chamber. The water tank is used for priming the pump at the begining of operation, and thereafter water is circulated through the cutting nozzle in a closed loop. The maximum coaxial water jet velocity that can be obtained is about 19 m/s, limited by the pump capacity. In the present study the effects of laser power, standoff distance (SOD) and water-jet velocity in cutting AISI 304 stainless steel (SS) sheets of 0.5 - 1.5 mm thickness have been studied. SS specimens of 160 mm x 100 mm dimensions were taken and 80 mm long straight slits were laser cut for different sets of process parameters to determine the kerf-width and taper. The cutting process was initiated after laser piercing in the sheet. The top and bottom surface kerf-widths were measured with an optical microscope having an eyepiece graticule of 10 μm least count. Full length laser cutting was also done at increasing cutting speeds to determine its maximum value at which specimen is just separated out and to study its parametric dependence.

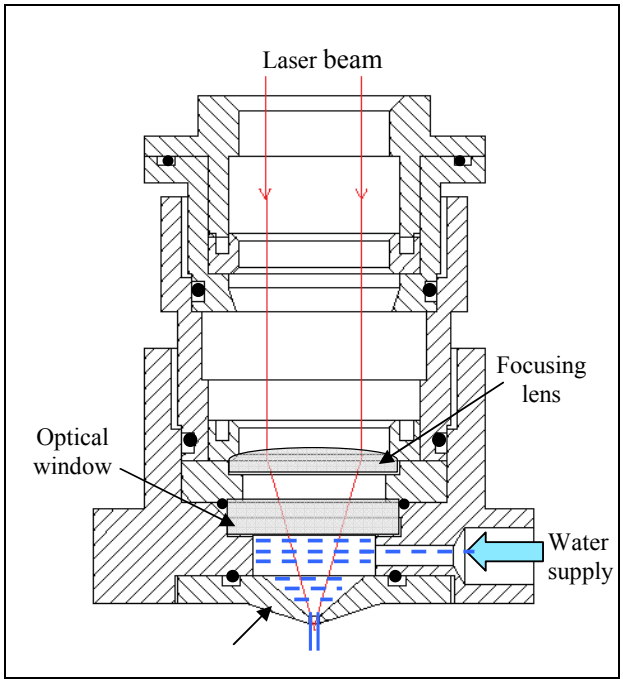

Fig. 1 Schematic of the cutting nozzle and transmission of laser beam through water

III. Experimental Results and Discussions

The water-jet assisted underwater laser cutting process was found to be remarkably gentle and produced very little turbulence in water compared to the gas assisted underwater cutting process. The basic mechanisms involved in this cutting process are the melting of work piece material by laser beam and the melt-ejection by coaxial water-jet. Fig. 2(a) shows the underwater laser cutting process of a 1 mm thick steel sheet with water-jet assist at 1800 W laser power. Gentle nature of the cutting process is evident from the relatively short length of the melt ejection shower compared to what is usually observed in a gas-assisted underwater laser cutting process [18]. For a comparison underwater laser cutting was also carried out using gas assist with this cutting head and the cutting process is shown in Fig. 2(b). It is apparent that the gas assisted underwater cutting process produces very high turbulence and gas bubbles in water compared to water-jet assisted cutting process. Some amount of water was vaporized at the laser-material-water interface in water-jet assisted laser

cutting process; however the bubbles so formed were readily swept away by the water jet. Some of these bubbles got condensed in the water which is at near room temperature and some escaped out of water.

The first set of laser cutting experiments was carried out to determine the maximum cutting speed for 0.5, 1.0 and 1.5 mm thick sheets at different laser powers at a constant standoff distance (SOD) of 1.0 mm and water-jet speed of 18 m/s. Fig. 3 shows the variation of the maximum cutting speed with laser power. This shows that the maximum cutting speed increased with laser power at constant water-jet speed and SOD, and the rate of increase was more for the thinner sheet.

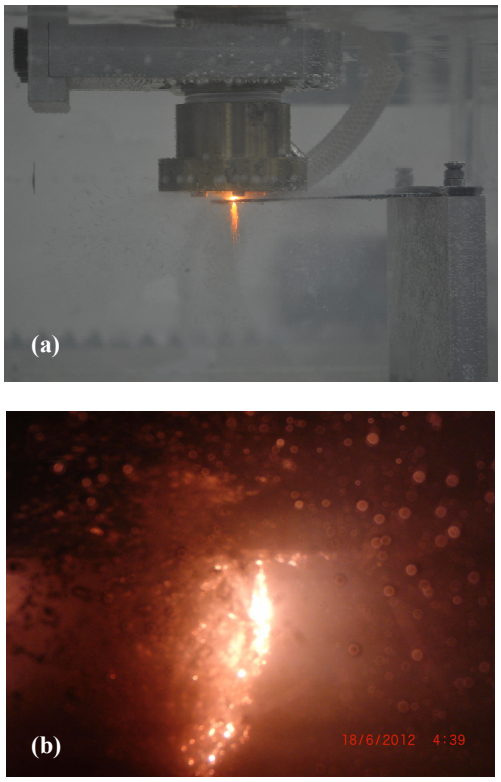

Fig. 2 Photograph of underwater laser cutting of 1 mm thick stainless steel sheet (a) water-jet assisted (b) gas assisted

In gas assisted laser cutting, severance energy expressed as $S = P_L/v.t$, where P_L is laser power, v is cutting speed and t is sheet thickness, is approximately constant for a material [24]. The estimation of severance energy at different laser powers in water-jet assisted underwater laser cutting indicated that its value decreased with increasing laser power and corresponding increase in cutting speed. In water-jet assisted laser cutting the convective heat loss by water-jet will be significant. Its contribution may reduce with increasing cutting speed. And, this could be the reason for the reduction in severance energy at higher cutting speeds.

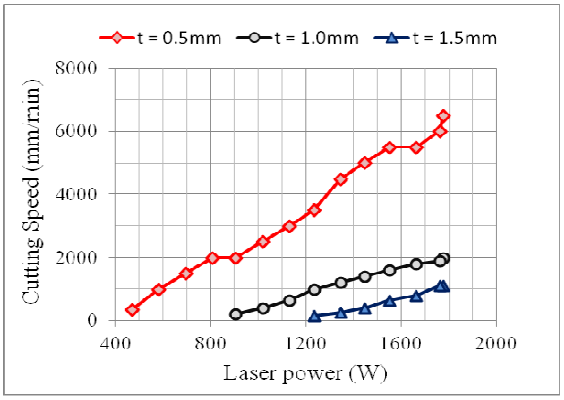

Fig. 3 Variation of cutting speed with laser power in SS sheet of different thicknesses at 1.0 mm SOD and 18 m/s water-jet speed

In the second set of experiments the effects of SOD and water-jet speed on the maximum cutting speed were studied in 1 mm thick sheet by varying SOD and water-jet speed in the range of 0.5 – 1.5 mm and 15 – 19 m/s respectively. The effect of SOD on cutting speed is presented in Fig. 4(a) for constant water-jet speed and different laser powers. The maximum cutting speed tended to reduce with the increase of SOD. However, this effect was more prominent at lower laser powers. This trend can be explained considering the increase in laser spot size with the increase of SOD and the decrease in heat loss at higher cutting speeds corresponding to higher laser powers. The focal point of the laser beam was at the work piece surface for SOD of 0.5 mm, and as SOD was increased beyond 0.5 mm, the laser spot diameter increased. Therefore, the maximum cutting speed decreased with increasing SOD at constant laser power. At higher laser powers, the maximum cutting speed increased for all sheet thicknesses and these resulted in the reduction of heat loss.

The effect of water-jet speed on the cutting speed was also investigated keeping SOD constant and no significant effect was observed within the range of water-jet speed of 15 - 19 m/s, Fig. 4 (b).

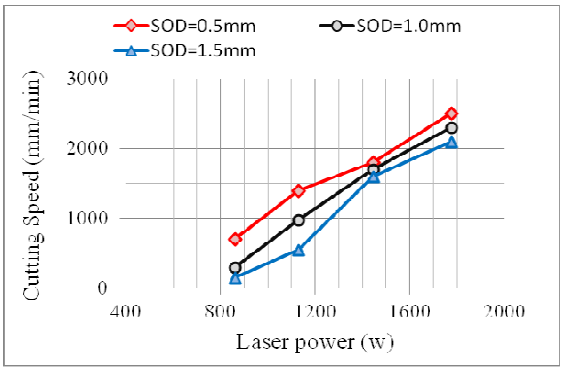

(a)

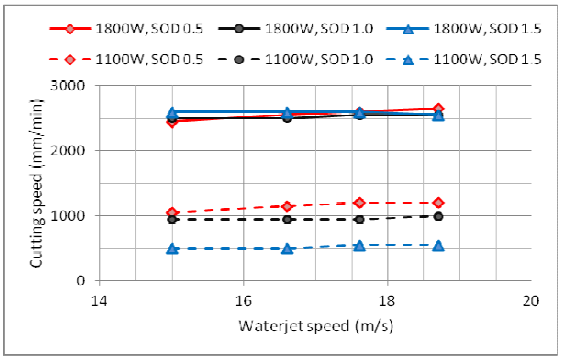

(b)

Fig. 4 Variation of cutting speed in 1 mm thick SS sheet with (a) laser power at 18 m/s water-jet speed for different SOD and, (b) water-jet speed for different laser power and SOD

In the third set of experiments the effects of laser power, cutting speed, SOD and water-jet speed on the kerf-width and striation pattern were studied. Fig. 5 shows the variation in the top and bottom surface kerf-widths with these processing parameters in 1 mm thick specimens. Both top and bottom surface kerf-widths increased with laser power at almost the same rate, Fig. 5 (a). With the increase in cutting speed, both the surface kerf-widths got reduced; but the bottom surface kerf-width reduced at a faster rate than the top surface kerf-width, Fig. 5 (b). With the increase in SOD, the top surface kerf-width increased and the bottom surface kerf-width decreased Fig. 5 (c). And, with the increase in water-jet velocity the trend was reversed, while the top surface kerf-width decreased, the bottom surface kerf-width increased, Fig. 5 (d).

The kerf-width at the top and bottom surfaces will depend on the laser beam diameter, laser power, laser dwell time, water jet velocity and also the divergence of the water-jet. The dwell time, t_d can be given by $t_d = d_b/v$, where d_b and v are the laser spot diameter and cutting speed respectively. The laser power density at the centre of a focused beam is maximum and decreases gradually along the radial direction. The rise in surface temperature, ΔT can be considered to be proportional to $(H_L.\sqrt{t_d})$ product, where H_L is the absorbed laser power density at the surface and t_d is the laser dwell time. The radial distance, r_m from the centre up to which this product will exceed the threshold for melting, molten material up to this radial distance will be ejected out by the shear pressure of water jet and this will determine the kerf-width. The increase in the top and bottom surface kerf-widths with increasing laser power (Fig. 5(a)) is due to the increase in $(H_L.\sqrt{t_d})$ product and corresponding increase in r_m. The increase in cutting speed, v reduces the $(H_L.\sqrt{t_d})$ product and this results in a reduction in r_m, which is reflected in the kerf-width, Fig. 5 (b). Moreover, as the cutting speed is increased, the cut-front tends to get more inclined from the laser beam direction and this will cause a reduction in the laser power reaching to the bottom surface [25]. This could be the reason for the higher reduction in the bottom surface kerf-width than that of the top surface with the increase of the cutting speed, Fig. 5 (b).

The increase in the top surface kerf-width with increasing SOD can be attributed to the increased laser spot diameter, Fig. 5 (c). And, the decrease in the bottom surface kerf-width (Fig. 5 (c)) could be due to the higher reduction in the shear pressure of water-jet at the bottom surface than at the top surface with the increase of SOD. In Fig. 5 (d), it is observed that the trends of variation in the top and bottom surface kerf-widths with the increase of water-jet speed are opposite.

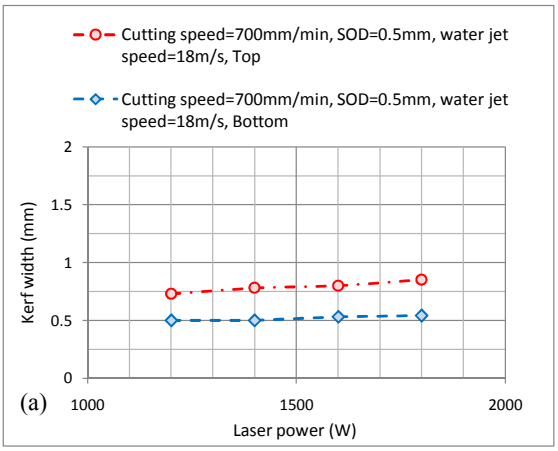

(a)

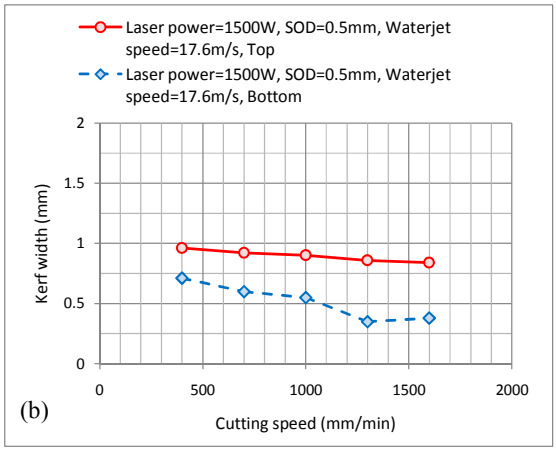

(b)

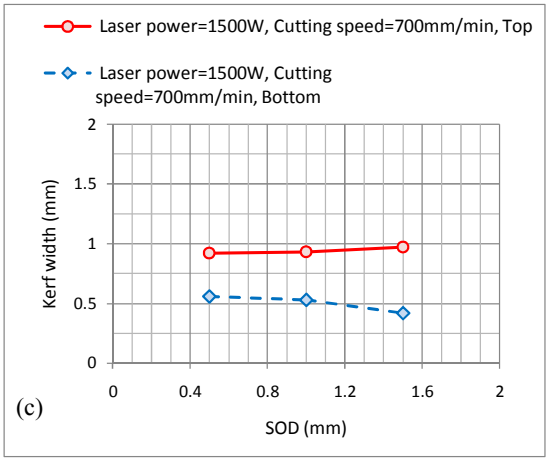

(c)

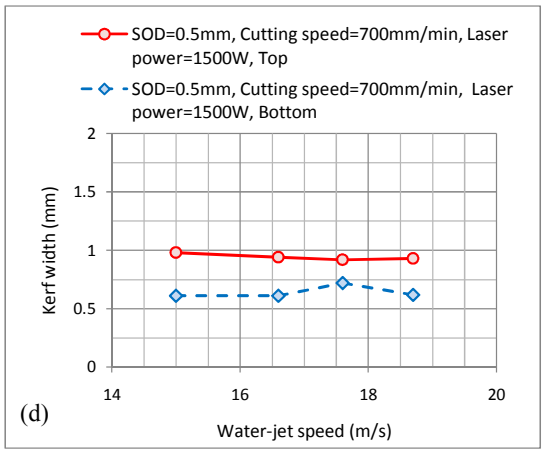

Fig. 5 Dependence of kerf width on (a) laser power, (b) cutting speed, (c) SOD and (d) water-jet speed

The increase in water jet speed can cause increased cooling and also impart higher shear pressure. While the enhanced cooling can cause a reduction in kerf-width, the higher shear pressure may produce a wider kerf-width. The opposite trends of Fig. 5 (d) could be because of the increased cooling effect dominating over the higher shear pressure effect with increasing water-jet velocity at the top surface and vice-versa at the bottom surface.

The macrographs of cut surfaces presented in Fig. 6 show the striation patterns at different cutting speeds in 1mm thick specimens. At a lower cutting speed the material removal was almost complete with a little dross sticking at the bottom edge, Fig. 6 (a), but at a higher cutting speed the molten material was not completely ejected and a lot of dross remained stuck at the bottom edge, Fig. 6 (c).

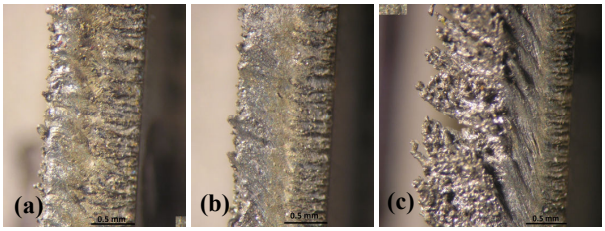

Fig. 6 Macrographs of cut surfaces at 1500 W laser power, 0.5 mm SOD, 18 m/s water-jet speed and different cutting speeds, (a) 400 mm/min, (b) 700 mm/min, (c) 1600 mm/min

The laser cut surface apparently has at least three striation patterns. Similar striation patterns have been reported in the gas-assisted laser cutting of steel and other alloyed sheets with CO_2, disk and fiber lasers [26]-[30]. The first top zone has nearly vertical striations and the material seems to be rapidly removed by vaporization and melt ejection, similar to the laser drilling process. Very little re-solidified material is observed here. The direct absorption of laser beam and heat diffusion determines mainly the thickness of melt layer and the movement of melting front in this zone. Vertical striations indicate that the influence of melt flow on the movement of melting front is negligible during the penetration of laser beam through the 1st zone [27]. In the present laser processing conditions, the surface temperature can reach to the boiling temperature within 80 µs and evaporation can set in. The rate of laser beam penetration can be of the order of 100 mm/s and during the time period of material removal up to the depth of 1st zone the work-piece will move by less than 80 µm. The extent of 1st zone along the direction of sheet thickness decreases with increasing cutting speed due to the reduction of the line energy (P_L/v). However, the striation wavelength remains almost invariant with the increase of cutting speed as reported by Poprawe and Koing [27]. In the 2nd zone striations are inclined and the inclination angle from the laser beam direction is found to increase with the increase of laser cutting speed. Scintilla and Tricarico [30] have also reported similar observations in the cutting of magnesium alloy with a fiber laser. In addition to the direct laser absorption and heat diffusion, the heat convection contributes to the melt layer thickness in this zone. The molten and semisolid material is removed by the shear pressure of water-jet in this zone causing relatively deeper striations compared to the first zone. The laser power reaching towards the bottom edge reduces especially at a higher cutting speed. As the molten material moves down along the sheet thickness it tends to cool down and becomes more viscous. The molten material may get re-solidified at the bottom edge before it is ejected out by the water-jet, Fig. 6 (c). Therefore, the third striation zone is characterized by the dominance of re-solidified molten material.

The specific laser energy to remove a unit volume of material and expressed as $Es = S/w = P_L/t.v.w$ was calculated for cutting with the maximum laser power for a particular sheet thickness, t and taking the average kerf-width, w; and was found to be in the range of 60-80 J/mm^3, increasing with higher sheet thickness. This is compared with the theoretically calculated [31] and experimental values [32] reported for the fiber laser cutting of stainless steel with nitrogen gas assist, which is in the range of 30 – 40 J/mm^3. The relatively higher specific energy may be due to the higher convection energy loss in water-jet and the scattering loss of laser light in water vapor generated at the laser-water-material interface.

Fig. 7 (a) and 7 (b) shows the laser scattering inside water before the laser beam strikes the workpiece and at the time of laser beam just striking the work-piece, respectively. Their comparison indicates that the scattering loss is relatively less when the laser beam has not struck the workpiece. But, when the laser beam strikes the work-piece various phenomena such as reflection and scattering of laser beam, heating, melting, and vaporization occur at the cutting front surface. The water vapor bobbles scatter the incoming laser beam and cause a reduction in the laser power reaching the workpiece.

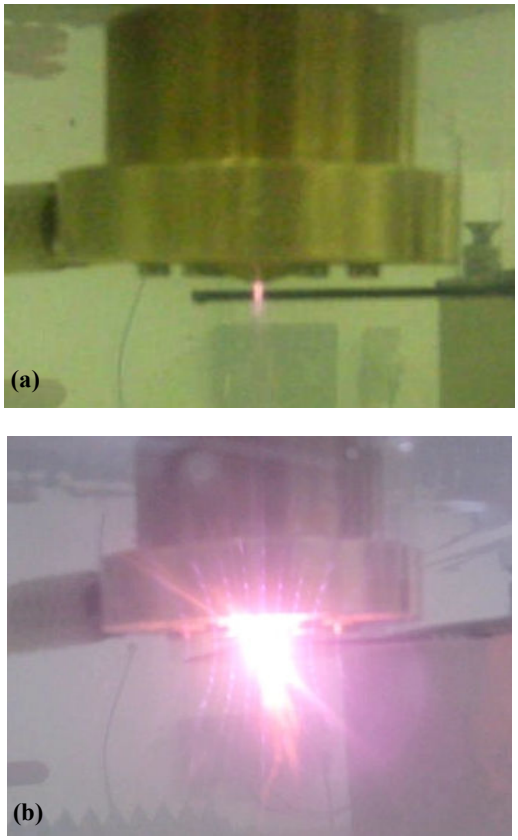

Fig. 7 Laser beam scattering in water-jet assisted underwater laser cutting process (a) before laser beam strikes the work piece and (b) at the time of laser beam striking the work piece

The underwater laser cutting of SS 304 with oxygen assist was also carried out for comparing the specific energy in the two underwater cutting processes. The specific energy was found to be in the range of 45 J/mm^3 in cutting 1 mm thick SS material at 1000 W laser power and it varied with the gas pressure. Thus, from the efficiency point of view the O_2 gas assisted underwater laser cutting process is better than the water-jet assisted underwater laser cutting process. However, it was observed that the heat affected zone and the spatter at the top surface is remarkably less in case of water-jet assisted cutting process.

The above experimental results and discussions reveal that the effects of various process parameters on the water-jet assisted underwater laser cutting performance is similar to that of the conventional gas assisted laser cutting, except that there is an additional energy loss due to the heat convection and scattering of laser light by water vapour bubbles. A lumped heat capacity model including various loss mecahnisms will be developed. Also, the effects of higher laser power density and higher water-jet velocity on the cutting performance, and different phenomena such as the formation and condensation of water vapor bubbles and scattering of laser radiation will be investigated further.

IV. Conclusion

In conclusion, a water-jet assisted underwater laser cutting process using a high power fiber laser has been demonstrated. This cutting process is relatively gentle, produces much less turbulence and gas bubbles in water compared to the gas-assisted underwater laser cutting process. AISI 304 steel sheets up to 1.5 mm thickness were cut by this process using a fiber laser at 1800 W laser power at a maximum cutting speed of 1.4 m/min with water-jet speed of 18 m/s. The effect of various processing parameters on the cutting performance are similar to the conventional gas assisted laser cutting characteristics; however, the convective heat loss by water-jet and the scattering of laser beam by water vapor cause a reduction in the process efficiency. The efficiency improves with increasing cutting speed at higher laser powers. This process may have potential application in underwater cutting of nuclear reactor components as this produces very less turbulence in water and aerosols in surrounding environment.

Acknowledgment

Authors gratefully acknowledge the financial supports from the Board of Research on Nuclear Science under Grant # 2009/34/33/BRNS/2752 dt 04/01/2010 and from the Department of Science and Technology, Government of India, under the FIST Program-2007(#SR/FIST/ETII-031/2007). They would like to thank Dr. A. K. Das, Dr. Shailesh Kumar and Mr. D. K. Shukla of Bhabha Atomic Research Centre, Mumbai for their interest in the work and many fruitful discussions.

References

[1] J. Lu, R. Q. Xu, X. Chen, Z. H. Shen, X. W. Ni, Mechanism of laser drilling of metal plates underwater, J. Appl. Phys., 95(8) (2004) 3890-3894.
[2] Chwan-Huei Tsai, Chang-Cheng Li, Investigation of underwater laser drilling for brittle substrates, J. Mater. Process. Tech., 209 (2009) 2838–2846.
[3] Y. Yan, L. Li, K. Sezer, W. Wang, D. Whitehead, L Ji, Y Baob, Y. Jiang, CO2 laser underwater machining of deep cavities in alumina, J. Eur. Ceram. Soc., 31 (2011) 2793–2807.
[4] K.L. Choo, Y. Ogawa, G. Kanbargi, V. Otra, L.M. Raff, R. Komanduri, Micromachining of silicon by short-pulse laser ablation in air and under water, Mater. Sci. Eng. A, 372 (2004) 145–162.
[5] A. K. Das, P. Saha, Excimer Laser Micromachining of Silicon in Air and Water Medium, Int. J. Manuf. Tech. Manag., 21(1-2) (2010) 42-53.
[6] L. M. Wee, E. Y. K. Ng, A. H. Prathama , H. Zheng, Micro-machining of silicon wafer in air and underwater, Opt. Laser. Technol., 43 (2011) 62–71.
[7] J.J.J. Kaakkunen, M. Silvennoinen, K. Paivasaari, P. Vahimaa, Water-Assisted Femtosecond Laser Pulse Ablation of High Aspect Ratio Holes, Physics Procedia, 12 (2011) 89–93.
[8] L.M. Wee, L. E. Khoong, C.W. Tan, and G. C. Lim, Solvent-Assisted Laser Drilling of Silicon Carbide, Int. J. Appl. Ceram. Technol., 8 [6] (2011)1263–1276.
[9] L. S. Jiao, E. Y. K. Ng , L. M. Wee, and H. Y. Zheng, The effect of assist liquid on the hole taper improvement in femtosecond laser percussion drilling, Physics Procedia, 19 (2011) 426–430.
[10] C. S. Montross, T. Wei, L. Ye, G. Clark, Y. W. Mai, Laser shock processing and its effects on microstructure and properties of metals: a review, Int. J. of fatigue, 24 (2002) 1021-1036.
[11] N. Muhammad, D. Whitehead, A. Boor, L. Li, Comparison of dry and wet fibre laser profile cutting of thin 316L stainless steel tubes for

medical device applications, J. Mater. Process. Tech., 210 (2010) 2261–2267.
[12] N. Muhammad, L. Li, Underwater femtosecond laser micromachining of thin nitinol tubes for medical coronary stent manufacture, Appl. Phys. A, 107 (2012) 849–861.
[13] B. Richerzhagen, R. Housh, F. Wagner, and J. Manley, Water jet guided laser cutting: a powerful hybrid technology for fine cutting and grooving, in Proceedings of the 2004 Advanced Laser Applications Conference and Exposition, D. Roessler and N. Uddin, eds. (ALAC, 2004), pp. 175–181.
[14] T. Levesqure, D. Perrottet, B. Richerzhagen, Damage-free cutting of medical devices using the water-jet-guided laser, Medical Devices Materials-III, ed. By Ramakroshna Venugopalanand Ming Wu, Proc. Materials and Processes for Medical Devices Conf., Nov. 14-16, 2005, Boston, Mass. USA.
[15] J. A. Porter, Y. A. Louhisalmi, J. A. Karjalainen, S. Füger, Cutting thin sheet metal with a water jet guided laser using various cutting distances, feed speeds and angles of incidence, Int. J. Adv. Manuf. Technol., 33 (2007) 961–967.
[16] V. Tangwarodomnukun, J. Wang, C.Z. Huang, H.T. Zhu, An investigaton of hybrid laser-waterjet ablation of silicon substrate, Int. j. Mach. Tool. Manu., 56 (2012) 39-49.
[17] I. Chida, K. Okazaki, S. Shima, K. Kurihara,Y. Yuguchi, I. Sato, Underwater cutting technology of thick stainless steel with YAG laser, Proc. SPIE 4831 (453) (2003), http://dx.doi.org/10.1117/12.497715.
[18] R. K. Jain, D. K. Agrawal, S. C. Vishwakarma, A. K. Choubey, B. N. Upadhyaya and S. M. Oak, Development of underwater laser cutting technique for steel and zircaloy for nuclear applications, Pramana, 75 (6) (2010) 1253-1258.
[19] T. Hino, M. Tamura, Y. Tanaka, W. Kouno, Y. Makino, S. Kawano, and K. Matsunaga, Development of Underwater Laser Cladding and Underwater Laser Seal Welding Techniques for Reactor Components, J. Power and Energy Systems, 3 (1) (2009) 51-59.
[20] A. Kruusing, Underwater and water-assisted laser processing:Part 2—Etching, cutting and rarely used methods, Opt. Laser Eng., 41(2) (2004) 329-352.
[21] J. A. Curcio and C. C. Petty, The Near Infrared Absorption Spectrum of Liquid Water, J. Opt. Soc. Am., 41(5) (1951) 302-304.
[22] S. Mullick, Y. K. Madhukar, S. Kumar, D. K. Shukla, and A. K. Nath, Temperature and intensity dependence of Yb-fiber laser light absorption in water, Appl. Opt., 50(34) (2011) 6319-6326.
[23] Y. K. Madhukar, S. Mullick, D. K. Shukla, S. Kumar, A. K. Nath, Effect of laser operating mode in paint removal with a fiber laser, Appl. Surf. Sci., 264 (2013) 892– 901.
[24] W. M. Steen and J. Mazumder, Laser Material Processing, 4th edition, Springer – Verlag London 2010, pp156-161.
[25] L. D. Scintilla, L. Tricarico, A. Wetzig, A. Mahrle, E. Beyer, Primary losses in disk and CO2 laser beam inert gas fusion cutting, J. Mate. Process. Tech., 211 (2011) 2050–2061.
[26] A. Bharti, R Sivakumar, The mechanism of laser removal in laser fusion cutting, Laser Eng., 5(2) (1996) 87-105.
[27] R. Poprawe, W. König, Modeling, Monitoring and Control in High Quality Laser Cutting, CIRP Annals - Manufacturing Technology, 50(1) (2001) 137–140.
[28] R. Poprawe, W. Schulz, R. Schmitt, Hydrodynamics of material removal by melt expulsion: Prospectives of laser cutting and drilling, Physics Procedia5 (2010) 1–18.
[29] L. D. Scintilla, L.Tricarico , Estimating cutting front temperature difference in disk and CO2 laser beam fusion cutting, Opt. Laser Technol., 44 (2012) 1468–1479.
[30] L. D. Scintilla, L.Tricarico, Experimental investigation on fiber and CO2 inert gas fusion cutting of AZ31magnesium alloy sheets, Opt. Laser Technol., 46 (2012) 42-52.
[31] A. Mahrle and E. Beyer, Theoretical aspects of fibre laser cutting, J. Phys. D: Appl. Phys. 42 (2009) 175507 (9pp).
[32] K. Abdel Ghany, M. Newishy, Cutting of 1.2 mm thick austenitic stainless steel sheet using pulsed and CW Nd:YAG laser, J. Mate. Process. Tech., 168 (2005) 438–447.